The analysis of coffee-green tea-turmeric combination against cardiac-metabolic syndrome using metabolite profiling, gene expression, and *in silico* approach

[Análisis de la combinación de café, té verde y cúrcuma contra el síndrome cardiometabólico mediante perfiles de metabolitos, expresión génica y enfoque *in silico*]

Ermin Rachmawati[1,2]*, Mohammad S. Rohman[1,3]*, Nashi Widodo[1,4], Mifetika Lukitasari[1,5], Dwi A. Nugroho[1], Feri E. Hermanto[1,6,7], Mukhamad N. Kholis[1,2]

[1]Research Center for Cardiovascular, Brawijaya University, Malang, Indonesia.
[2]Department of Biomedical Sciences, Faculty of Medicine and Health Sciences, UIN Maulana Malik Ibrahim Malang, East Java, Indonesia.
[3]Department of Cardiology and Vascular Medicine, Faculty of Medicine, Universitas Brawijaya, Malang, Indonesia.
[4]Department of Biology, Faculty of Mathematics and Natural Sciences, Universitas Brawijaya, Malang, Indonesia.
[5]School of Nursing, Faculty of Health Sciences, Universitas Brawijaya, Malang, Indonesia.
[6]Faculty of Animal Sciences, Universitas Brawijaya, Malang, Indonesia.
[7]Bioinformatics Research Center, Indonesian Institute of Bioinformatics, Malang, Indonesia.
*E-mail address: ermin.rachmawati@kedokteran.uin-malang.ac.id, ippoenk@ub.ac.id

Abstract

Context: The development of functional drinks to inhibit oxidative stress and inflammation as a critical process in inducing heart damage in metabolic syndrome is required. Coffee, tea, and turmeric have all been shown to offer health advantages.

Aims: To investigate the effect of coffee, green tea, turmeric extract (ECGTT) against cardiac-metabolic syndrome (MetS).

Methods: The secondary metabolites from coffee, green tea, and turmeric were identified using LC-HRMS. Male Sprague–Dawley rats were divided into four groups (n = 4) representing normal, MetS, MetS with ECGTT treatment doses: 300/100/150 mg/BW and 300/100/250 mg/BW group. Upon the end of treatment periods, expression of tumor necrosis factor-alpha (TNFα), interleukin-6 (IL-6), nuclear factor kappa B (NF-κB), NADPH oxidase (NOX$_2$), SERCA2a were measured from the heart. A computational approach including network pharmacology, protein-protein interaction (PPI) network, molecular docking, and dynamic was performed to understand the molecular mechanism of ECGTT against cardiac damage in MetS.

Results: Chlorogenic acid (CGA), epigallocatechin gallate (EGCG), and curcumin were identified as the main metabolites in ECGTT. The ECGTT administration decreased the TNFα, IL-6, NF-κB, and NOX$_2$ and increased *SERCA2a* expression($p<0.05$). Moreover, the PPI result suggested that angiotensin II receptor type 1 (AGTR1) was the key regulator of cardiac injury-MetS induced. CGA, EGCG, and curcumin bind to AGTR1 with smaller binding energy than metformin and showed stability of structure and interaction among those metabolites into AGTR1.

Conclusions: Coffee, green tea, and turmeric might prevent heart dysfunction in MetS through modulation of oxidative stress and inflammation.

Keywords: calcium handling; coffee; green tea; inflammation; oxidative stress; turmeric.

Resumen

Contexto: Se requiere el desarrollo de bebidas funcionales para inhibir el estrés oxidativo y la inflamación como proceso crítico en la inducción del daño cardiaco en el síndrome metabólico. Se ha demostrado que el café, el té y la cúrcuma ofrecen ventajas para la salud.

Objetivos: Investigar el efecto del extracto de café, té verde y cúrcuma (ECGTT) contra el síndrome cardiometabólico (MetS).

Métodos: Se identificaron los metabolitos secundarios del café, el té verde y la cúrcuma mediante LC-HRMS. Las ratas macho Sprague-Dawley se dividieron en cuatro grupos (n = 4) que representaban los grupos normal, MetS, MetS con dosis de tratamiento ECGTT: 300/100/150 mg de peso corporal y 300/100/250 mg de peso corporal. Al final de los periodos de tratamiento, se midió en el corazón la expresión del factor de necrosis tumoral alfa (TNFα), la interleucina-6 (IL-6), el factor nuclear kappa B (NF-κB), la NADPH oxidasa (NOX$_2$) y la SERCA2a. Se realizó un enfoque computacional que incluía farmacología de red, red de interacción proteína-proteína (PPI), acoplamiento molecular y dinámica para comprender el mecanismo molecular de ECGTT contra el daño cardíaco en MetS.

Resultados: El ácido clorogénico (CGA), el galato de epigalocatequina (EGCG) y la curcumina se identificaron como los principales metabolitos en ECGTT. La administración de ECGTT redujo el TNFα, IL-6, NF-κB y NOX$_2$ y aumentó la expresión de SERCA2a ($p<0,05$). Además, el resultado de la IPP sugirió que el receptor de angiotensina II tipo 1 (AGTR1) era el regulador clave de la lesión cardiaca inducida por MetS. CGA, EGCG y la curcumina se unen a AGTR1 con menor energía de unión que la metformina y mostró la estabilidad de la estructura y la interacción entre los metabolitos en AGTR1.

Conclusiones: El café, el té verde y la cúrcuma podrían prevenir la disfunción cardiaca en MetS a través de la modulación del estrés oxidativo y la inflamación.

Palabras Clave: café; cúrcuma; estrés oxidativo; inflamación; manejo del calcio; té verde.

Abbreviation: AGTR1: angiotensin II receptor type 1; CGA: chlorogenic acid); ECGTT: extract of coffee, green tea, turmeric; EGCG: epigallocatechin gallate; ESI: electron spray ionization; $FADH_2$: flavin adenine dinucleotide; FFA: free fatty acid; HDL: high density lipoprotein; HFHS: high fat high sucrose; IL-6: interleukin-6; KEGG: Kyoto encyclopedia of genes and genomes; LC-HRMS: liquid chromatography high resolution mass spectrophotometry; MetS: metabolic syndrome; MAPK: mitogen-activated protein kinase; NADH: nicotinamide adenine dinucleotide hydrogen; NADPH: nicotinamide adenine dinucleotide phosphate; NF-κB: nuclear factor kappa B; NOX_2: NADPH oxidase 2; PCR: polymerase chain reaction; PPARγ: peroxisome proliferator activated receptor gamma; PPI: protein-protein interaction; RMSD: root-mean-square deviation; RMSF: root-mean-square fluctuation; ROS: reactive oxygen species; SEM: standard error of mean; SERCA2a: sarcoplasmic reticulum calcium adenosine triphosphatase; STZ: streptozotocin; TNFα: tumor necrosis factor.

INTRODUCTION

The burst of oxidative stress and chronic low-grade inflammation interact to induce heart dysfunction in uncontrolled metabolic syndrome (MetS) (D'Oria et al., 2020; Wang et al., 2021). In chronic low-grade inflammation, the high activity of nicotinamide adenine dinucleotide phosphate (NADPH) oxidase induces the defect in myocardial calcium handling as the early marker of cardiac contractility dysfunction in MetS (Battault et al., 2020). It can manifest as cardiomyopathy or even heart failure.

Numerous reports showed that the cardiovascular complication of MetS is rising globally, although efforts to prevent this disease have been continuously implemented worldwide (Alshehri, 2010). Due to MetS patients' poor adherence to healthy lifestyles and consuming metformin as primary medicine to limit the progression of MetS (Burnier and Egan, 2019), it is an emerging issue to develop any strategies to overcome the problem. Considering the holistic treatment concept and advantages of multi-target, multi-link, and multi-approach, natural product use has been widely valued in recent years as a prevention strategy to inhibit the progression of MetS (Patti et al., 2018). Based on previous reports, the use of coffee and green tea extract showed evidence to be developed as a functional drink to inhibit the progression of MetS (Rachmawati et al., 2021; 2022). Chlorogenic acid (CGA) in coffee and catechins in green tea have antioxidant and anti-inflammatory effects (Lau et al., 2016). Interestingly, several studies demonstrated that the combination of coffee and green tea could lower blood pressure, fasting blood glucose levels, and weight loss and showed anti-atherosclerotic capacity through modulation of metabolic gene expression (Lukitasari et al., 2020).

Unfortunately, a high concentration of epigallocatechin gallate (EGCG), the main active ingredient in green tea, could induce liver toxicity. Shi et al. (2021) reported that EGCG at concentrations of 400 and 800 mg/kg BW lowered the number of hepatocytes due to high levels of apoptosis and vacuolar degeneration, infiltration of inflammatory cells in mice under dietary restriction. Moreover, a randomized, double-blind, placebo-controlled clinical trial of 538 participants showed liver function abnormalities after consuming EGCG 843 mg/day for 12 months (Shi et al.,

2021; Yu et al., 2017). The liver injury caused by high dose of EGCG can be explained by the prooxidant effect, the decline of glutathione level, reduced mitochondrial membrane potential collapse and damage of outer mitochondrial membrane, which leads to hepatic necrosis and inflammation (Kucera et al., 2015).

This study tried to add turmeric, which is hepatoprotective, to minimize the side effects of EGCG (Pan et al., 2014; Saleh et al., 2021). Khan et al. (2019) showed that turmeric hepatoprotective properties have been investigated in several hepatotoxicity protocols. Besides hepatoprotective activities, turmeric could be cardioprotective. However, no study has tried to reveal the 3-combination effect in preventing calcium handling abnormalities in heart MetS. Calcium handling dysfunction has been characterized by the lower activity and expression of sarcoplasmic reticulum calcium adenosine triphosphatase (SERCA2a), which is regulated by oxidative stress due to MetS (Balderas-Villalobos et al., 2013; Calvert, 2014; Tang et al., 2010).

The recent study evaluated the cardioprotective effect of coffee, tea, and turmeric against cardiotoxicity, emphasizing inflammation, NADPH oxidase, and calcium dysregulation handling. The *in vivo* approach would like to see the transcriptional modulation of inflammation and oxidative stress, which thus might control the SERCA2a expression after being treated with the combination of coffee/tea/turmeric extract. To obtain a wider perspective, we also performed an *in silico* study analyzing the networking pharmacology of coffee, green tea, and turmeric in cardiovascular disease associated with MetS. Thus, the result was used for identifying the possible target marker of coffee, tea, and turmeric active compounds in the signal transduction cascades.

MATERIAL AND METHODS

Preparation of coffee-green tea-turmeric extract

Coffea canephora var. *robusta* (L. Linden) A. Chev. beans were retrieved from Dampit Coffee Plantation Malang Indonesia (8°44'16.64"S,113°41'52.26"E). The *Camellia sinensis* (L.) Kuntze leaves were collected from Ciwidey, Indonesia (7°9'24.48"S, 108°0'23.4"E). *Curcuma longa* L. *syn. Curcuma domestica* Valeton was

retrieved from UPT Materia Medica Batu Malang, Indonesia (7°52'1.811"S, 112°31'15.196"E). The green coffee bean and green tea leaves were deposited as an example in the Molecular Biology Laboratory at Universitas Brawijaya with the reference numbers KAD-001 and TSN-506801, respectively. The *Curcuma longa* L. syn. *Curcuma domestica* Valeton reference number was 2011.06.KNT.L.R.005.

The green coffee bean (*Coffea canephora var. robusta*) was roasted until the temperature reached 180°C, and the crack sound appeared in an automatic coffee roaster (N500i). Subsequently, the lightly roasted coffee bean was ground into powder and then macerated in ethanol 95% (Lukitasari et al., 2020). A rotary evaporator (RV10 autoV, IKA) set at 40°C was used to remove the ethanol from the coffee (Lukitasari et al., 2020). On the other hand, after the green tea leaves (*Camellia sinensis*) dried at 50°C for 8 h, the green tea was boiled for 30 min at 80°C. The sundried turmeric powder (*Curcuma longa*) was boiled using mineral water at 90°C for 49 min. Liquid and solid phases of coffee, green tea, and turmeric infusions were filtered using Whatman paper 4. Identification of active ingredients was completed using the LC-HRMS method.

The selection of coffee, green tea, and turmeric (ECGTT) extract combination concentration for *in vivo* study: 300/100/150 mg/kg BW (group 1) and 300/100/250 mg/kg BW (group 2) were based on a previous study by Esmaeelpanah et al. (2021).

Liquid Chromatography High-Resolution Mass Spectrophotometry (LC-HRMS) analysis

The extract was further processed for identification of bioactive compounds by LC-HRMS (LTQ XL, Thermo Electron Corporation, USA) analysis. The detection was performed through direct injection mode with an Electron Spray Ionization (ESI) probe at positive mode. The flow rate of the sample was kept at 8 µL/min, while the capillary temperature was set at 280°C. The mass was in the range from 50 to 1000 m/z. As a mobile phase, the ratio of methanol and acetonitrile was 80:20 (v/v). The MS parameters for each compound were optimized to ensure the most favorable ionization and ion transfer conditions and attained the optimum signal of both the precursor and fragment ions by infusing the analytes and manually turning the parameters. The source parameters were identical for all the analytes (Khan et al., 2017).

Animal and experimental design

The *in vivo* study evaluated the gene expression of oxidative stress and inflammation markers. 24 male Sprague–Dawley rats (age 9 weeks) were purchased

from the Indonesian National Agency of Drug and Food Control. This experimental design and protocols have been approved by the Health Research Ethics Committee of Saiful Anwar General Hospital, Malang, Indonesia, by registered number 400/211/K.3/302/2021. The Replacement, Reduction, and Refinement (3R) principles were used in all experiment processes. The animal care in all experimental procedures was under the rigorous supervision of the ethical commission. This study used the minimum number of rats, and appropriate measures were taken to minimize pain or discomfort.

First, rats were housed and acclimatized for 7 days in an ecologically controlled standard polycarbonate cage sized 50 cm × 30 cm × 15 cm with hemp bedding at a temperature of 25°C in 40%–70% relative humidity and 12:12 h light-dark cycle environment. They were maintained with food AIN-93M and drank *ad libitum*. Food was provided and replaced daily.

After 7 days of the acclimatization process, the rats were randomized into a normal that received a standard diet (n = 6) and High Fat High Sucrose (HFHS) diet group as MetS model (n = 18). On the second week of the protocol, the HFHS rats were injected intraperitoneally using streptozotocin (STZ) (bioWORLD cat.41910012-4) (30 mg/ kg). On the eighth week of protocol, the rats were categorized as MetS based on NCEP-ATP III if they fulfilled three minimum criteria as follows: (1) fasting blood glucose levels over 126 mg/dL, (2) triglyceride level over 150 mg/dL, (3) systolic blood pressure over 140 mmHg, and (4) High-Density Lipoprotein (HDL) cholesterol lower than 40 mg/dL. Thus, the HFHS groups were divided into a negative control group that supplemented with HFHS diet (n = 6), HFHS + ECGTT 100/300/150 (n = 6) and ECGTT 100/300/250 mg/kg BW group (n = 6), respectively. After 17 weeks of treatment, the rats were sacrificed by cervical decapitation (Rohman et al., 2017).

Gene expression quantification

The heart was immediately removed after decapitation and kept in an RNA buffer solution to maintain the integrity of the RNA. The total RNA was extracted using the Total RNA Extraction Kit easy-BLUE (Intron Biotechnology, South Korea) reagent and was kept at -80°C until gene expression analysis. The ReverTra Ace- kit was used to execute the cDNA synthesis (Ref FSK-101, Toyobo, Japan). Light Cycler 96 equipment was used to perform polymerase chain reaction (PCR, Takara, Japan). Each tube of the PCR mixture contained the specific primers, cDNA, and GoTaq Master Mix (Ref M7122, Promega, Madison, USA) (Integrated DNA Technologies, Singapore). The

following primers were created using NCBI Primer-BLAST.

NF-κB	Forward 5′-AACGCATCCCAAGGTGCTGGA-3′
	Reverse 5′-GCAGCTGGAAAAGCTCAAGCCA-3′
TNFa	Forward 5′-CGTCAGCCGATTTGCCATTTC-3′
	Reverse 5′-TGGGCTCATACCAGGGCTTG-3′
Il-6	Forward 5′-CCCAACTTCCAATGCTCTCCTAAT-3′
	Reverse 5′-GCA CAC TAG GTT TGC CGA GTA GA-3′
NOX₂	Forward 5′-TGACTCGGTTGGCTGGCATC-3′
	Reverse 5′-CGCAAAGGTACAGGAACATGGG-3′
β-actin	Forward 5′-CGAGTACAACCTTCTTGCAG-3′
	Reverse 5′-CATTGTAGAAAGTGTGGTGC-3′

The polymerase chain reaction (PCR) amplification protocol consisted of 5 min at 95°C for pre-denaturation, 10 cycles of denaturing at 95°C for 30 s, annealing at 60°C for 30 s, and extension at 72°C for 30 s. This was followed by a further 30 cycles of denaturing at 95°C for 30 s, annealing at any temperature derived from melting temperature reduced by 5C for 30 s, and extension at 72°C for 30 s. The reaction was held at 4°C. The product of PCR was electrophoresed using Mupid-exU Submarine Electrophoresis System (Advance, Japan) and was captured by using ImageQuant LAS 500 Chemiluminescence CCD Camera (Guangdong Denley Technology, China). All bands were semi-quantified using ImageJ as the relative expression level of each gene after normalization to the housekeeping gene (β-actin).

Network pharmacology, protein-protein interaction (PPI) network construction and module analysis

A pharmacological network is an approach to identifying the work of drug candidates by identifying multiple targets in a disease. Cytoscape is a JavaScript library for interactive network visualization by identifying CGA, EGCG, and curcumin target genes that are critical in diabetic cardiomyopathy pathogenesis.

The first step in performing network pharmacology was defining a list of genes involved in cardiovascular disease associated with MetS. Thus, the genes involved in diabetic cardiomyopathy were extracted from the Disgenet database (https://www.disgenet.org/). Besides that, the extraction of the gene targets of CGA, EGCG, and curcumin as coffee, tea, and turmeric main ingredients were also collected using the Pubchem database (https://pubchem.ncbi.nlm.nih.gov/). Subsequently, the network pharmacology was analyzed using Cytoscape 3.9.1 software (Su et al., 2015). The identified genes from the previous steps were merged. Similar

results of genes from two categories and their interaction were visualized.

Similar genes from network pharmacology were used in PPI analysis to get a comprehensive overview of protein interaction (Szklarczyk et al., 2015). The PPI network was constructed using STRING v11.0 (Search Tool for the Retrieval of Interacting Genes/Proteins) (https://string-db.org/) with a median confidence score was set >0.4. The outcome was determined with the biological processes and Kyoto Encyclopedia of Genes and Genomes (KEGG) pathways related to protein interaction in the PPI network with a significant p-value of <0.05 (Szklarczyk et al., 2015).

Molecular docking

The CGA (CID 1794427), EGCG (CID 65064), and curcumin (CID 969516) were selected as the ligands that might have an important role in inhibiting inflammation and stress oxidative stress by acting competitively with the native ligand. Prior to docking, the chemical ligands were saved as SDF files. The control used for site-specific docking was metformin (Pubchem ID 4091).

Angiotensin receptor 1 (AGTR1) was selected as the receptor for a specific docking process based on the KEGG Pathway from Cytoscape and PPI network analysis. The RCSB Protein Data Bank (http://www.rcsb.org) provided the crystal structure of the extracellular domain of AGTR1 (PDB ID 4YAY). Prior to docking, water molecules, the presence of native ligands, and non-standard residues were removed and left only polar hydrogen. All of this process were executed using Biovia Discovery Studio. The energy of the optimized structure was then minimized to eliminate steric conflicts between the atoms. After fixing all of these issues, the structure file was put into AutoDock Tools and added as a macromolecule (Ferreira et al., 2015).

AutoDock Vina was used to dock angiotensin receptor 1 with EGCG, CGA, and curcumin. Binding site of AGTR1 was comprised of Arg167, Trp84, and Tyr35, Phe77, Tyr87, Ser105, Val108, Ser109, Leu112, Ala163, Phe182, Ile288, and Tyr292. The grid box's center was determined based on the location of the active site region. The center: X = -16,5144; Y = 12,901; Z = 42,438. Dimension (Amstrong): X = 18,9913, Y = 25,5764; Z = 24,2872. (Ferreira et al., 2015).

Molecular dynamics simulations

YASARA version 19.12.14 was employed to perform the molecular dynamics simulations (Gogoi et al., 2021). The simulation settings were set as physiological milieu as in the previous experiment, i.e., 310°K of temperature, 1 bar of pressure, 0.9% NaCl

concentration, 0.997 water density, and 50 ns simulation periods. All simulations were performed under the AMBER14 force field. The Root-Mean-Square Deviation (RMSD) and Root-Mean-Square Fluctuation (RMSF) from the simulation analysis determined the structural stability of each simulated complex.

Data and statistical analysis

The parameters from the *in vivo* study were presented as mean ± standard error of the mean (SEM). The evidence of the extract to influence the parameters was performed using SPSS 26. The differences in groups were examined using an ANOVA one-way test with a confidence level of 95% as significant at $p \leq 0.05$. The evaluation of any difference among groups was performed by LSD test.

RESULTS

The LC-HRMS analysis

The peak chromatogram of coffee, green tea, and turmeric from LC-HRMS demonstrated the possible candidate compounds. The list of phytoconstituents of LC-HRMS is shown in Table 1 and Fig. 1. The CGA, EGCG, and curcumin were identified as the main secondary metabolites of coffee, green tea, and turmeric, respectively.

The effect of coffee, green tea, and turmeric extract combination lowering the oxidative stress marker NOX_2, inflammation marker NF-κB, TNFα, IL-6 and increase SERCA2a expression in heart-rat MetS model

One complication of MetS was observed mainly in the cardiovascular system. An early marker of cardiac complication induced by MetS is the disruption of the calcium handling signaling pathway, which was characterized by a decreased expression of SERCA2a due to inflammation and oxidative stress. In this experiment, the rats supplemented with the HFHS diet were treated with two concentrations of ECGTT (100/300/150 mg/kg BW and 100/300/250 mg/kg BW). Inflammatory marker expression (TNFα, IL-6, NF-κB), oxidative stress (NOX_2), and SERCA2a expression were analyzed in the rat heart after the complete experiment. Fig. 2 shows that these extract combinations could lower TNFα, IL-6, NF-κB (p=0.000), NOX_2 (p=0.003), and increase the SERCA2a (p=0.000) expression in rats MetS model supplemented with coffee, green tea, and turmeric extract.

There was a significant difference between the control group, MetS, and the treatment group for *NF-κB*, *IL-6* gene expression. Administration of this combination significantly decreased *NOX_2* expression.

Even at an ECGTT dose of 100/300/250 mg/kg BW, *NOX_2* expression was lower than NOX_2 expression in the control rat group. The relative expression of *SERCA2a* was higher in the coffee, green tea, and turmeric groups than in the control group.

Pharmacology network

A total of 220 genes were retrieved from the Disgenet database for diabetic cardiomyopathy. On the other hand, the number of genes identified as targets of EGCG, CGA, and curcumin was 2764, 201, and 2538, respectively. Fig. 3 demonstrates the edges that reflect the interaction pathway between the botanical group, active ingredients, gene targets of the phytoconstituent, and diabetic cardiomyopathy.

There were 265 nodes, 342 edges, average number of neighbors 2581, network diameter 6, network radius 3, characteristic plastic length 3167; network density 0.010, network heterogeneity 40994; network centralization 0.402 from Cytoscape report analysis. The overlapping genes from the botanical group and genes from diabetes cardiomyopathy were selected using Venn analysis as a source for conducting the PPI network. 4 common elements found in "EGCG", "CGA", "CURCUMIN" and "DIABETIC": CASP3, IL-1B, TNF, BCL2; 3 common elements in "EGCG" and "DIABETIC": IGF1R, KLF4, SLC2A1. 8 common elements in "EGCG", "CURCUMIN" and "DIABETIC": CRP, CTNNB1, IL10, MAPK1, MAPK3, SIRT1, TGFB1, TP53; 33 common elements in "CURCUMIN" and "DIABETIC": ACE, ACE2, ADIPOQ, AGER, AGT, AGTR1, AKT1, BAD, CASP8, CXCL8, EGF, EGFR, FN1, GSK3B, HMOX1, INS, KEAP1, MIR34A, MMP9, NFE2L2, NPPA, OPA1, PARP1, PRKCD, PPARG, SIRT3, SMAD2, SPP1, STAT3, TLR2, TNNI3, VEGFA, XDH.

A total of 48 genes were used for the PPI network constructed on the STRING database. The resultant network had 47 nodes and 631 edges (Fig. 4B). The functional analysis of the PPI network obtained 84 KEGG Pathway, where 10 might related to metabolic complications to the heart, as shown in Table 1. After that, we searched for membrane protein receptor that contributes to heart complication, which links to SERCA2a or calcium regulation, inflammation, and oxidative stress. We found AGTR1 might have a vital role in facilitating the pathological process, as seen in hsa-04933 and 04020 (Fig. 4C).

The CGA, EGCG, and curcumin potency to block signaling pathways related to AGTR1

Based on the pathways from the previous result, AGTR1 was involved in the upstream molecule that could activate the expression of NOX_2 and also linked

to inflammation in cardiomyocytes. Thus, this protein is suitable to be used as an important target for EGCG, CGA, and curcumin to lower the myocardium complication due to MetS. It was proposed that these active compounds could blockade the signaling pathway triggered by this receptor. Therefore, in order to get a comprehensive prediction of the combination work, this study analyses the binding affinity value of three chemical substances with AGTR1 using control metformin and statin. The position of interaction and the amino acid residues in the receptor contact with the ligand are shown in Fig. 5A.

The protein-protein docking is mainly guided by the hydrogen bonding and hydrophobic effect. The interaction between CGA, EGCG, and curcumin with AGTR1 is shown in Fig. 5A. In addition, Table 2 describes the hydrogen and hydrophobic contacts of CGA, EGCG, and curcumin with AGTR1. The data showed the same amino acid residues of CGA and/or EGCG and/or curcumin with the native ligand of AGTR1 as follows: ARG167, TRP84, VAL108, TYR 34, TYR 92, and ILE 288. Our findings demonstrated that

CGA, EGCG, and curcumin binding affinity were more negative than metformin, which determined these active constituents to be more stable than the standard drug.

Complete prediction about EGCG, CGA, and curcumin interaction in AGTR1 was analyzed using molecular dynamics simulation. The RMSD of the atom backbone showed a stable structure in all of the simulated complexes, including AGTR1-metformin (Fig. 5B). The stability of each complex was also justified by the RMSF of each residue. No significant difference was found in the fluctuation of every residue in each complex (Fig. 5C). From the ligand point of view, the structure of EGCG, CGA, and curcumin displayed more stable conformation upon binding with the AGTR 1 than metformin (Fig. 5D). The movement of those compounds as the ligand also minimum, showed by the RMSD of the ligand movement (Fig. 5E). Thus, molecular dynamics simulation revealed a stable interaction of each complex to perform an inhibitory activity against AGTR1.

Table 1. Binding affinity and amino acid residues, which are responsible for ligand and receptor contacts.

Description	FDR value	Genes	p-value	Term name
AGE-RAGE signaling pathway in diabetic complications	$8.16E^{-27}$	MAPK1|TGFB1|SMAD2|MAPK3|IL1B|STAT3|CXCL8|CASP3|FN1|AGT|AGER|PRKCD|MAPK8|BCL2|TNF|AGTR1|AKT1|VEGFA	$4.86E^{-29}$	hsa04933
Fluid shear stress and atherosclerosis	$9.53E^{-15}$	KEAP1|HMOX1|IL1B|TP53|CTNNB1|MMP9|MAPK8|NFE2L2|BCL2|TNF|AKT1|VEGF A	$4.08E^{-16}$	hsa05418
HIF-1 signaling pathway	$3.77E^{-14}$	MAPK1|HMOX1|MAPK3|STAT3|EGF|EGFR|NPPA|INS|BCL2|AKT1|VEGFA	$2.36E^{-15}$	hsa04066
FOXOs signaling pathway	$2.11E^{-13}$	SIRT1|MAPK1|TGFB1|MAPK3|STAT3|EGF|EGFR|MAPK8|INS|IL10|AKT1	$1.51E^{-14}$	hsa04068
Type II diabetes mellitus	$2.51E^{-10}$	MAPK1|MAPK3|PRKCD|MAPK8|INS|ADIP OQ|TNF	$3.44E^{-11}$	hsa04930
Calcium signaling pathway	$2.53E^{-10}$	MAPK1|MAPK3|EGF|EGFR|GSK3B|BAD|M APK8|AKT1	$3.55E^{-11}$	hsa04012
Phospholipase D signaling pathway	$6.06E^{-10}$	MAPK1|MAPK3|EGF|EGFR|CXCL8|AGT|INS|AGTR1|AKT1	$8.66E^{-11}$	hsa04072
Insulin resistance	$1.50E^{-09}$	STAT3|GSK3B|AGT|PRKCD|MAPK8|INS|T NF|AKT1	$2.37E^{-10}$	hsa04931
cGMP-PKG signaling pathway	$4.69E^{-07}$	MAPK1|MAPK3|NPPA|BAD|INS|AGTR1|A KT1	$1.26E^{-07}$	hsa04022
Renin-angiotensin system	$1.5 8E^{-06}$	ACE|AGT|ACE2|AGTR1	$4.47E^{-07}$	hsa04614
JAK-STAT signaling pathway	$7.6 1E^{-06}$	STAT3|EGF|EGFR|BCL2|IL10|AKT1	$2.38E^{-06}$	hsa04630
Hypertrophic cardiomyopathy	$8.45E^{-06}$	TGFB1|ACE|TNNI3|AGT|TNF	$2.67E^{-06}$	hsa05410
TGF-beta signaling pathway	$9.20E^{-06}$	MAPK1|TGFB1|SMAD2|MAPK3|TNF	$2.96E^{-06}$	hsa04350
NF-kappa B signaling pathway	$1.47E^{-05}$	IL1B|CXCL8|PARP1|BCL2|TNF	$4.82E^{-06}$	hsa04064
Regulation of actin cytoskeleton	$3.18E^{-05}$	MAPK1|MAPK3|EGF|EGFR|FN1|INS	$1.05E^{-05}$	hsa04810
Type I diabetes mellitus	$3.50E^{-04}$	IL1B|INS|TNF	$1.30E^{-04}$	hsa04940

Figure 1. Total ion and single chromatogram of ECGTT based on LC-HRMS analysis.

The peak indicates the possible metabolite from coffee **(A)**, green tea **(B)**, and turmeric extract **(C)**. The single chromatogram with a green highlight shows the predicted active ingredient found in the extract.

ECGTT: Extract of Coffee-Green Tea-Turmeric; LC-HRMS: Liquid Chromatography High-Resolution Mass Spectrophotometry. Data are expressed with the prediction of secondary metabolite inside the LC-HRMS.
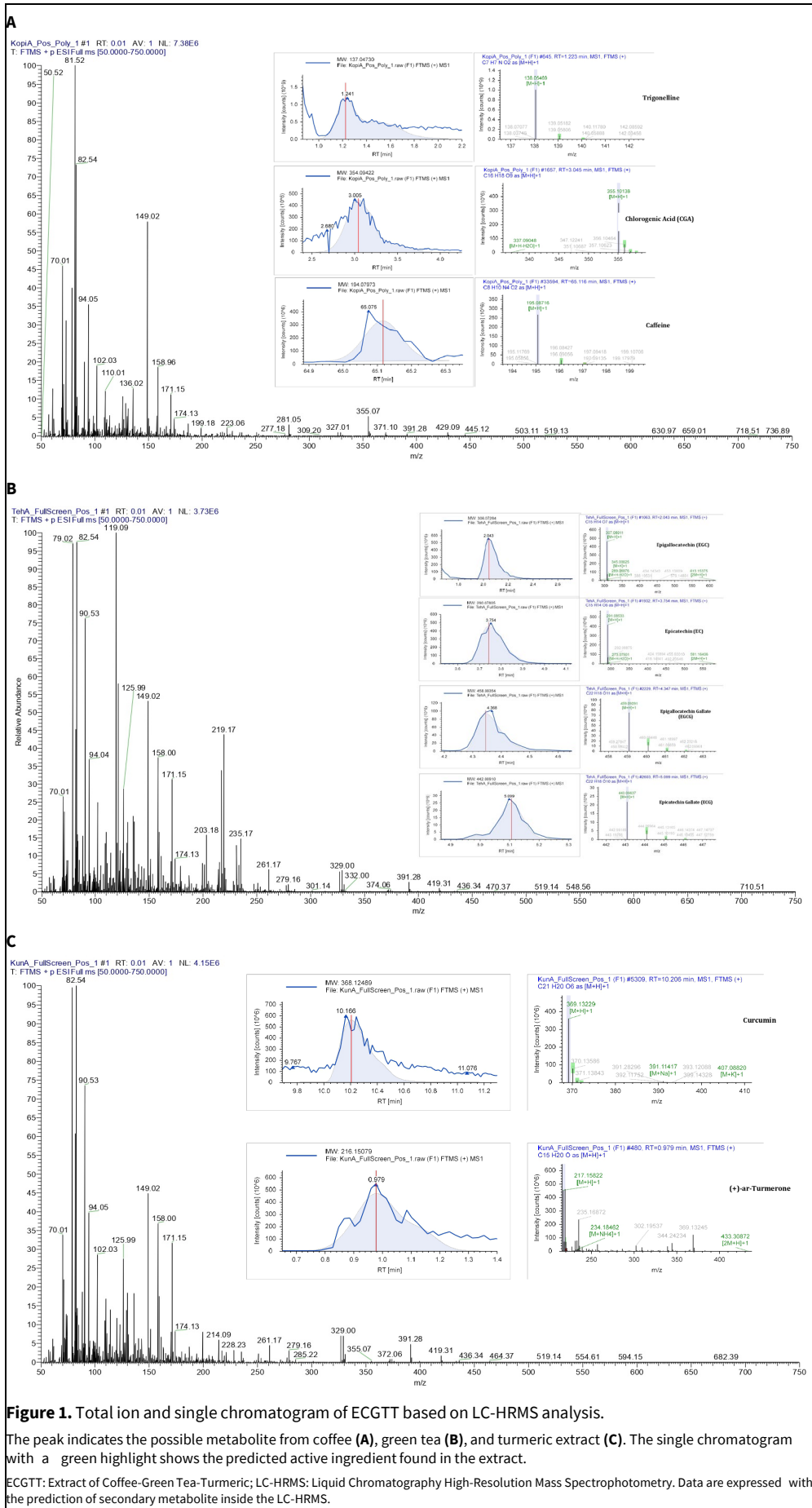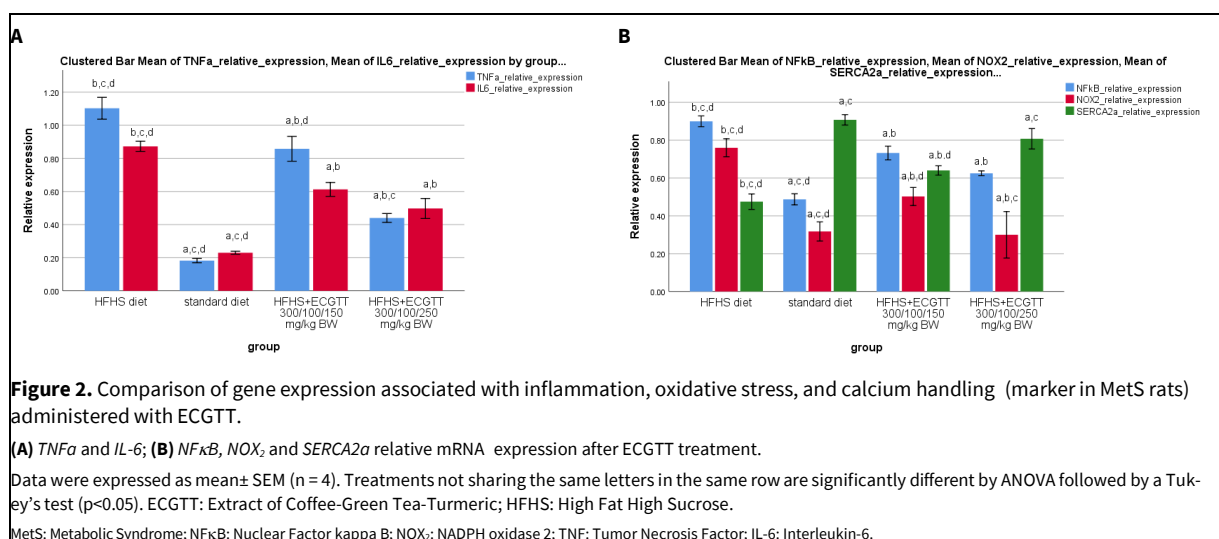
Table 2. Binding affinity and amino acid residues that are responsible for ligand and receptor contacts.

Receptor	PubChem ID	Active compound	Binding affinity (kcal/L)	Bonds
AGTR1	4091	Metformin	-5.1	**Hydrogen bonds**: TYR35, TRP 84
				Hydrophobic contacts: -
	65064	EGCG	-8.6	**Hydrogen bonds:** ARG167, TYR92
				Hydrophobic contacts: VAL108, TRP 84, MET 284; ILE A:288
	1794427	CGA	-7.9	**Hydrogen bonds:** TRP84, THR88, ARG167, ALA21
				Hydrophobic contact: TYR92
	969516	Curcumin	-7.6	**Hydrogen bonds:** TRP84, ARG167, TYR92
				Hydrophobic contact: PRO285, MET284, ILE288, VAL108, TYR 35

AGTR1: Angiotensin Receptor Type 1; EGCG: Epigallocatechin gallate; CGA: Chlorogenic acid.

Figure 2. Comparison of gene expression associated with inflammation, oxidative stress, and calcium handling (marker in MetS rats) administered with ECGTT.

(A) *TNFα* and *IL-6*; **(B)** *NFκB, NOX₂* and *SERCA2α* relative mRNA expression after ECGTT treatment.

Data were expressed as mean± SEM (n = 4). Treatments not sharing the same letters in the same row are significantly different by ANOVA followed by a Tukey's test (p<0.05). ECGTT: Extract of Coffee-Green Tea-Turmeric; HFHS: High Fat High Sucrose.

MetS: Metabolic Syndrome; NFκB: Nuclear Factor kappa B; NOX₂: NADPH oxidase 2; TNF: Tumor Necrosis Factor; IL-6: Interleukin-6.

DISCUSSION

The high number of oxidative stresses in the cardiac MetS results from the upregulation of NADPH oxidase, especially NOX$_2$, and low subgrade chronic inflammation (D'Oria et al., 2020). The myocardium of rats supplemented with a high-fat diet (HFD) had 1.8-fold increases in reactive oxygen species (ROS) production and NOX$_2$ expression. Besides that, the increase in cardiomyocyte size, a sign of cardiac hypertrophy, was also observed. An increased free fatty acid (FFA) flux occurs under hyperglycemic conditions, followed by an increase of nicotinamide adenine dinucleotide hydrogen (NADH) and flavin adenine dinucleotide (FADH$_2$) formation and the overproduction of ROS. Furthermore, oxidative stress plays a critical role in the development of pathological remodeling and hypertrophy, as well as heart failure (D'Oria et al., 2020; de Geest and Mishra et al., 2022). However, these dysregulations were greatly

diminished in NOX$_2$ knock-out hearts (Bhatti and Li, 2020).

Pathological cardiac hypertrophy, marked by fibrosis and apoptosis, is linked to cardiac dysfunction due to MetS. Before the cardiac structure alteration manifests, the abnormality of calcium handling gene expression is observed, modulated by inflammation (Ly et al., 2017). Evidence comes from Villegas et al. (2000), which used a culture of new-born rat ventricular myocytes transfected with a 3.2 kb promoter plasmid construct that included the SERCA2 promoter coupled to a CAT reporter gene and treated with 10 ng/mL IL-6, showed that IL-6 dramatically reduced the activity of the SERCA2a promoter. In addition, a Western analysis using a polyclonal antibody to SERCA2 protein revealed a significant 60% reduction in the total quantity of SERCA2 protein in cultured myocytes (Villegas et al., 2000).
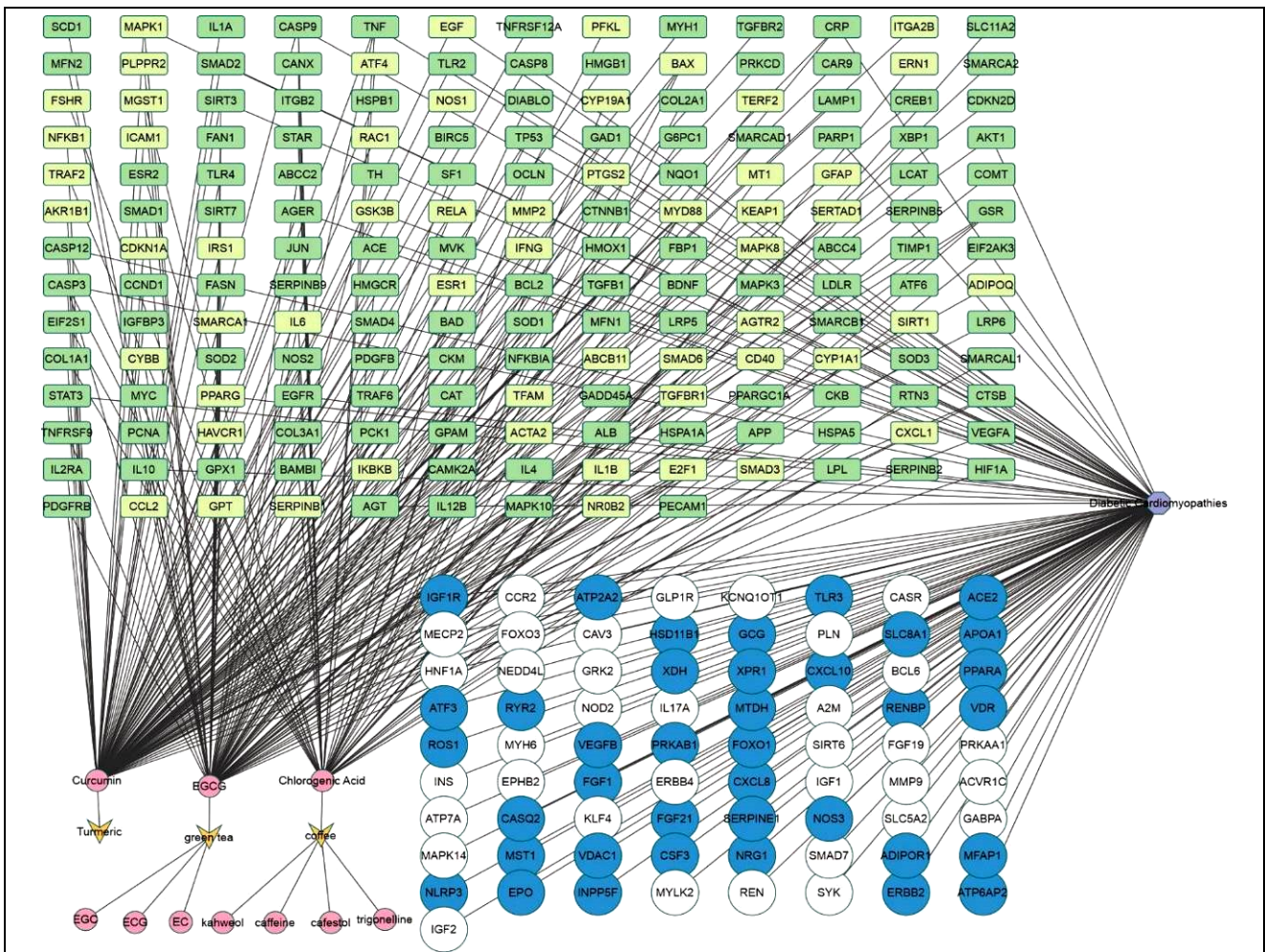
Figure 3. Visualization of the pharmacological network of coffee, green tea, and turmeric with cardiac dysfunction associated with MetS.

Orange arrows represent the botanical group. Pink circles represent the active ingredients of each botanical. Blue and white circles represent the gene target associated with botanical active ingredients and also the diseases. The green box represents the targets of the diabetic cardiomyopathy gene, which has also been identified as a target of CGA, EGCG, and turmeric (n = 178). Based on Cytoscape results, it was found that there was an association between CGA, EGCG, turmeric, and diabetic cardiomyopathy.

A2M: Alpha-2-Macroglobulin; ABCC2: ATP-Binding Cassette Sub-family C; ACE: Angiotensin-Converting Enzyme; ACE2: Angiotensin-Converting Enzyme 2; ACTA2: Actin Alfa 2; ACVR1C: Activin A Receptor Type 1C; ADIPOR2: Adiponectin Receptor 2; AKR1B1: Aldo-Keto Reductase Family 1, Member B1; APOA1: Apolipoprotein A1; ATF3: Activating Transcription Factor 3; ATF4: Activator of Transcription Factor-4; ATP2A2: ATPase Sarcoplasmic/Endoplasmic Reticulum Ca²⁺ Transporting 2; ATP6AP2: ATPase H+ Transporting Accessory Protein 2; BAD: Bcl-2 Associated Death Molecule; BAMBI: The Bone Morphogenetic Protein (BMP) and Activin Membrane-Bound Inhibitor; BAX: Bcl-2 Associated X-Protein; BCL2: B-Cell Lymphoma 2; BCL6: B-Cell Lymphoma 6; BDNF: Brain-Derived Neurotrophic Factor; CAMK2A: Calcium/calmodulin-Dependent Protein Kinase 2; CANX: Calnexin; CASP12: Caspase 12; CASP3: Caspase 3; CASP9: CRISPR Associated Protein 9; CASQ2: Calsequestrin 2; CAV3: Caveolin 3; CCL2: Chemokine Ligand 2; CCND1: Cyclin D1; CCR2: C-C Chemokine Receptor Type 2; CDKN1A: Cyclin-Dependent Kinase Inhibitor 1A; CKB: Creatine Kinase B; CKM: Cdk8 Kinase M-Type; COL1A1: Collagen Type 1; COL2A1: Collagen Type II Alpha 1 Chain; COL3A1: Collagen Type III Alpha 1 Chain; COMT: Catechol-O-Methyltransferase; CREB1: cAMP-Responsive Element-Binding Protein 1; CSF3: Colony Stimulating Factor 3; CTSB: Cathepsin B; CYBB: Cytochrome B, subunit B; CXCL8: C-X-C Motif Chemokine Ligand 8; CXCL10: C-X-C Motif Chemokine Ligand 10; EGF: Epidermal Growth Factor; EGFR: Epidermal Growth Factor Receptor; EIF2S1: Eukaryotic Translation Initiation Factor 2 Subunit Alpha; EPHB2: Ephrin type-B receptor 2; EPO: Endogenous Erythropoietin; ERBB4: Erb-B2 Receptor Tyrosine Kinase 4; ESR2: Estrogen Receptor 2; FAN1: Fanconi-Associated Nuclease 1; FASN: Fatty Acid Synthase; FGF19: Fibroblast Growth Factor 19; FGF21: Fibroblast Growth Factor 21; FOXO3: Forkhead Box O3; FSHR: Follicle Stimulating Hormone Receptor; GABPA: GA Binding Protein Transcription Factor Subunit Alpha; GAD1: Glutamic Acid Decarboxylase 1; GCG: Glucagon; GLP1R: Glucagon Like Peptide-1 Receptor Agonist; GPT: Glutamate Pyruvate Transaminase; GPX1: Glutathione Peroxidase; GRK2: G-Protein-Coupled Receptor Kinase 2; GSK3B: Glycogen Synthase Kinase 3B; GSR: Glutathione Reductase; HAVCR1: Hepatitis A Virus Cellular Receptor 1; HIF1A: Hypoxia Inducible Factor 1 alpha; HMGB2: High-Mobility Group Box 1 Protein; HMGCR: 3-Hidroxy-3-methylglutaryl-CoA Reductase; HMOX1: Heme Oxygenase-1; HNF1A: Hepatocyte Nuclear Factor-1 Alpha; HSD11B1: 11β-Hydroxysteroid Dehydrogenase Type 1; HSPA1A: Heat Shock Protein A 1; HSPB1: Heat Shock Protein Family B; ICAM1: Intercellular Cell Adhesion Molecule 1; IFNG: Interferon Gamma; IGF2: Insulin Like Growth Factor 2; IGFBP3: Insulin-Like Growth Factor Binding Protein 3; IGF1R: Insulinlike Growth Factor 1 Receptor; IKBKB: IkB Kinase Beta; IL10: Interleukin-10; IL12B: Interleukin-12B; IL1A: Interleukin-1A; IL2RA: Interleukin Receptor Subunit α; IL6: Interleukin-6; INPP5F: Inositol Polyphosphate-5-Phosphatase Factor; INS: Insulin; IRS1: Insulin Substrate Receptor 1; ITGB2: Integrin Beta 2; KCNQ1OT1: KCNQ1 Opposite Strand/Antisense Transcript 1; KLF4: Kruppel Family of Transcription Factors 4; LDLR: Low-Density Lipoprotein Receptor; LCAT: Lecithin Cholesterol Acyltransferase; LPL: Lipoprotein Lipase; LRP5:Llipoprotein Receptor 5; MAPK1: Mitogen-Actived Protein Kinase 1; MAPK10: Mitogen Activated Protein Kinase 10; MAPK14: Mitogen-Actived Protein Kinase 14; MECP2: Methyl CpG Binding Protein 2; MFAP1: Microfibril Associated Protein 1; MFN1: Mitofusins 1; MFN2: Mitofusin 2; MGST1: Microsomal Glutathione S-transferase 1; MMP2: Mtrix Metalloproteinase 2; MMP9: Matrix Metalloproteinase 9; MTDH: Metaderhin; MST1: Macrophage Stimulating 1; MYB: Myeloblastosis; MYD88: Myeloid Differentiation 88; MYLK2: Myosin Light Chain Kinase 2; MYH1: Myosin-1; MYH6: Myosin Heavy Chain 6; NEDD4L: Neural Precursor Cell Expressed Developmentally Downregulated Gene 4-Like; NF-κB: Nuclear Factor Kappa B; NLRP3: NLR Family Pyrin Domain Containing 3; NRG1: Neuregulin 1; NOD2: Nucleotide-Binding Oligomerization Domain-Containing Protein 2; NOS2: Nitrite Oxide Synthase 2; NOS3: Nitrite Oxide Synthase 3; NQO1: NAD(P)H Quinone Oxidoreductase 1; OCLN: Occludin; PCK1: Phosphoenolpyruvate Carboxykinase 1; PCNA: Proliferating Cell Nuclear Antigen; PDGFB: Platelet-Derived Growth Factor B; PDGFRB: Platelet-Derived Growth Factor Receptor B; PECAM1: Platelet Endothelial Cell Adhesion Membrane; PLN: Phospholamban; PLPPR2: Phospholipid Phosphatase Related 2; PPARG: Peroxisome Proliferator Activation Receptor Gene; PPARA: Peroxisome Proliferator Activated Receptor Alpha; PRKAB1: Protein Kinase, AMP-Activated, Beta 1 Non-Catalytic Subunit 1; PRKAA1: Protein Kinase AMP-Activated Catalytic Subunit Alpha 1; PTGS2: Prostaglandin-Endoperoxide Synthase-2; RAC1: Ras-Related C3 Botulinum Toxin Substrate 1; REN: Renin; RENBP: Renin Binding Protein; ROS1: Receptor Tyrosine Kinase 1; RYR2: Ryanodine Receptor 2; SCD1: Stearoyl CoA Desaturase 1; SERPINB8/9: SERPIN Family B Member 8/9; SF1: Steroidogenic Factor 1; SIRT1/3: Silent Information Regulator Sirtuin 1/3/7; SIRT6: Sirtuin 6; SLC5A2: Solute Carrier Family 5 Member 2; SLC8A1: Solute Carrier Family 8 Member A1; SMAD7: SMAD Family Member 7; SMARCA1: SWI/SNF Related, Matrix Associated, Actin Dependent Regulator of Chromatin, Subfamily A; SOD1/2: Superoxide Dismutase ½ ; STAR: Steroidogenic Acute Regulatory Protein; STAT3: Signal Transducer and Activator of Transcription 3; SYK: Spleen Associated Tyrosine Kinase; TH: Tyrosine Hydroxylase; TLR3: Toll Like Receptor 3; TLR4: Toll Like Receptor 4; TNF: Tumor Necrosis Factor; TNFRAF2: TNF Receptor Associated Factor 2; TNFRSF9: TNF Receptor Super Family member 9; TP53: Tumor Protein 53; TRAF6: TNF Receptor-Associated Factor 6; VDAC1: Voltage-Dependent Anion-Selective Channel 1; VDR: Vitamin D Receptor; VEGFA: Vascular Endothelial Growth Factor; VEGFB: Vascular Endothelial Growth Factor B; XBP1: X-Box Binding Protein 1; XDH: Xanthine Dehydrogenase; XPR1: Xenotropic and Polytropic Retrovirus Receptor 1.
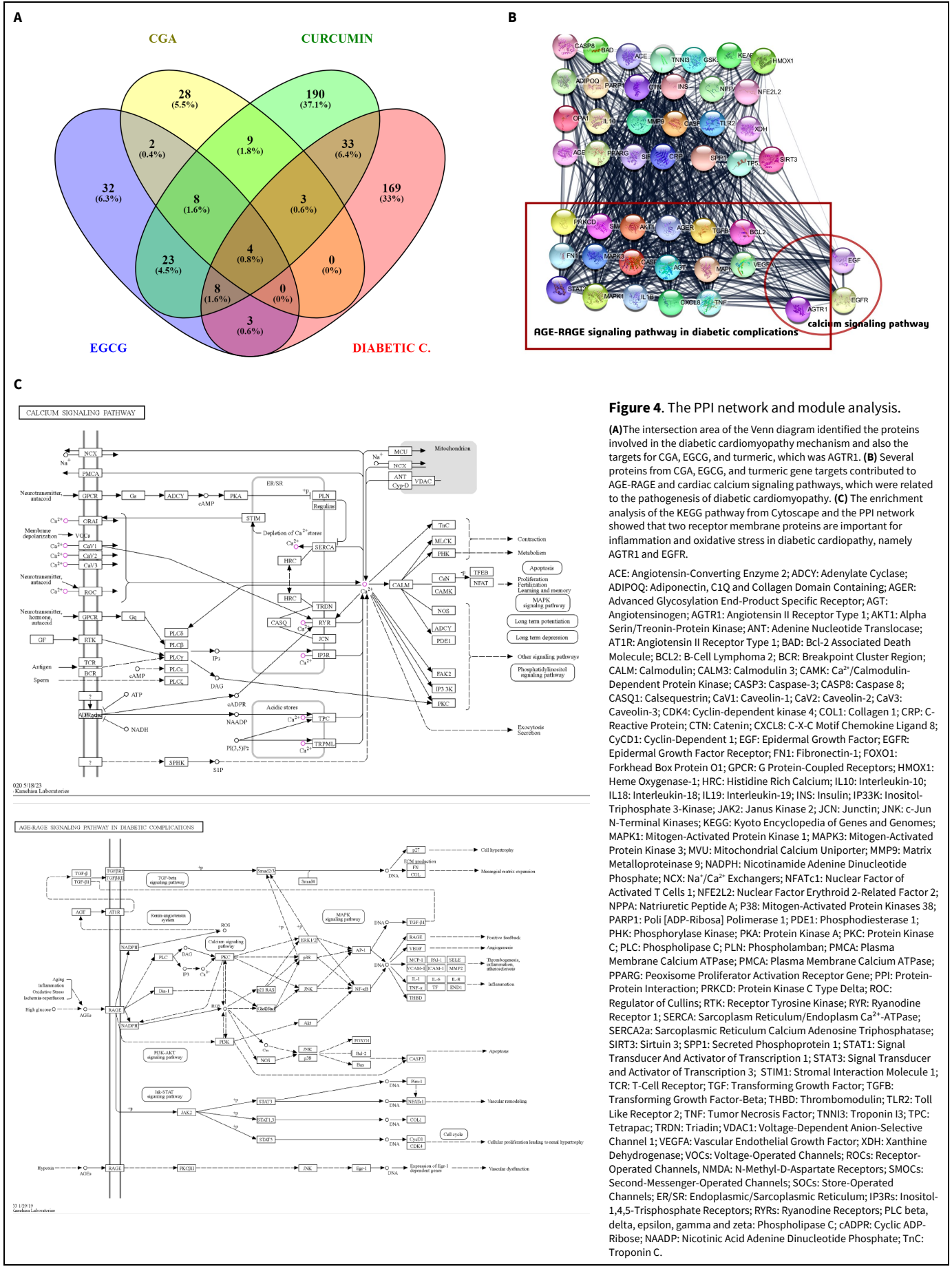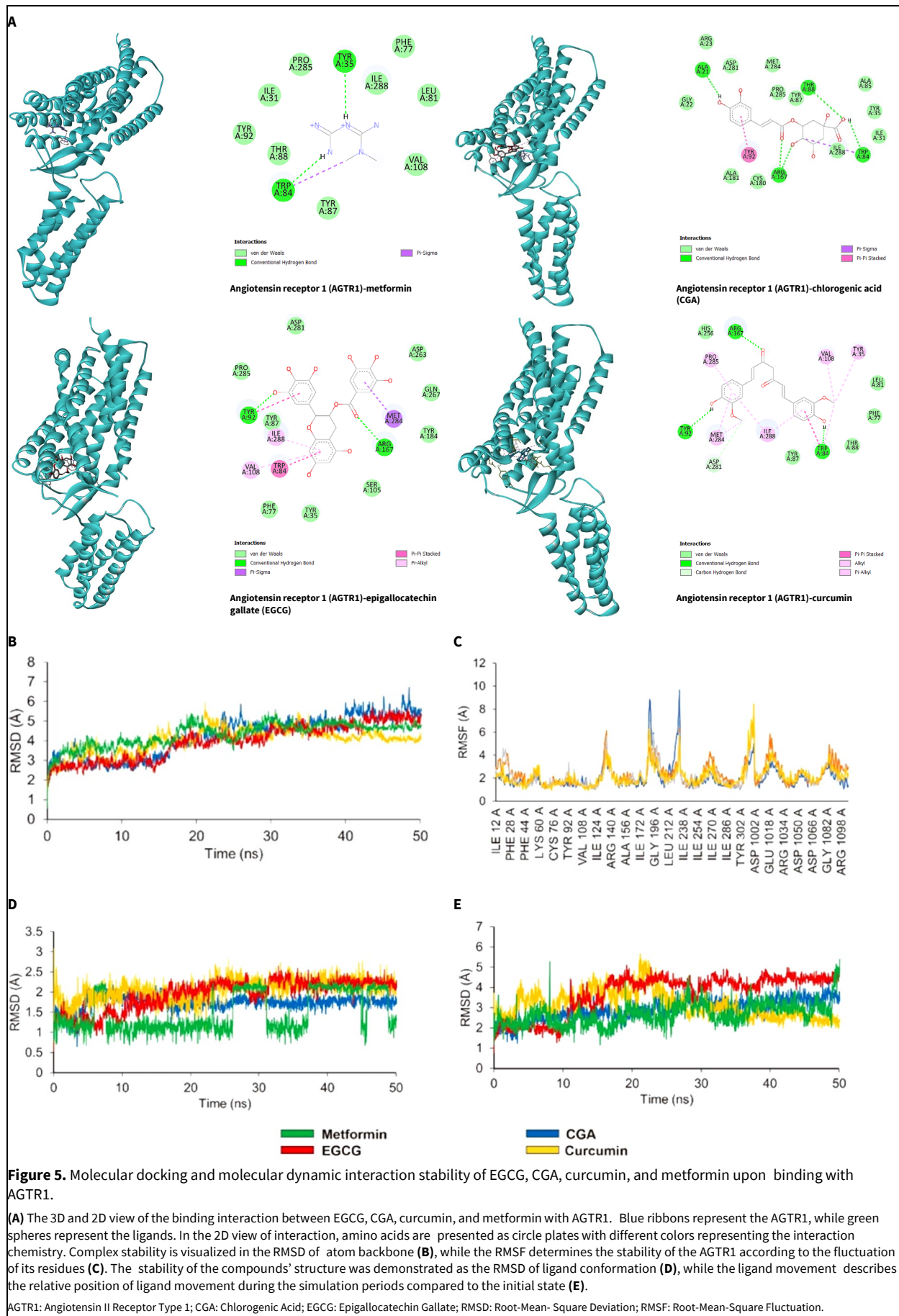
Figure 4. The PPI network and module analysis.

(A) The intersection area of the Venn diagram identified the proteins involved in the diabetic cardiomyopathy mechanism and also the targets for CGA, EGCG, and turmeric, which was AGTR1. **(B)** Several proteins from CGA, EGCG, and turmeric gene targets contributed to AGE-RAGE and cardiac calcium signaling pathways, which were related to the pathogenesis of diabetic cardiomyopathy. **(C)** The enrichment analysis of the KEGG pathway from Cytoscape and the PPI network showed that two receptor membrane proteins are important for inflammation and oxidative stress in diabetic cardiopathy, namely AGTR1 and EGFR.

ACE: Angiotensin-Converting Enzyme 2; ADCY: Adenylate Cyclase; ADIPOQ: Adiponectin, C1Q and Collagen Domain Containing; AGER: Advanced Glycosylation End-Product Specific Receptor; AGT: Angiotensinogen; AGTR1: Angiotensin II Receptor Type 1; AKT1: Alpha Serin/Treonin-Protein Kinase; ANT: Adenine Nucleotide Translocase; AT1R: Angiotensin II Receptor Type 1; BAD: Bcl-2 Associated Death Molecule; BCL2: B-Cell Lymphoma 2; BCR: Breakpoint Cluster Region; CALM: Calmodulin; CALM3: Calmodulin 3; CAMK: Ca²⁺/Calmodulin-Dependent Protein Kinase; CASP3: Caspase-3; CASP8: Caspase 8; CASQ1: Calsequestrin; CaV1: Caveolin-1; CaV2: Caveolin-2; CaV3: Caveolin-3; CDK4: Cyclin-dependent kinase 4; COL1: Collagen 1; CRP: C-Reactive Protein; CTN: Catenin; CXCL8: C-X-C Motif Chemokine Ligand 8; CyCD1: Cyclin-Dependent; EGF: Epidermal Growth Factor; EGFR: Epidermal Growth Factor Receptor; FN1: Fibronectin-1; FOXO1: Forkhead Box Protein O1; GPCR: G Protein-Coupled Receptors; HMOX1: Heme Oxygenase-1; HRC: Histidine Rich Calcium; IL10: Interleukin-10; IL18: Interleukin-18; IL19: Interleukin-19; INS: Insulin; IP33K: Inositol-Triphosphate 3-Kinase; JAK2: Janus Kinase 2; JCN: Junctin; JNK: c-Jun N-Terminal Kinases; KEGG: Kyoto Encyclopedia of Genes and Genomes; MAPK1: Mitogen-Activated Protein Kinase 1; MAPK3: Mitogen-Activated Protein Kinase 3; MVU: Mitochondrial Calcium Uniporter; MMP9: Matrix Metalloproteinase 9; NADPH: Nicotinamide Adenine Dinucleotide Phosphate; NCX: Na⁺/Ca²⁺ Exchangers; NFATc1: Nuclear Factor of Activated T Cells 1; NFE2L2: Nuclear Factor Erythroid 2-Related Factor 2; NPPA: Natriuretic Peptide A; P38: Mitogen-Activated Protein Kinases 38; PARP1: Poli [ADP-Ribosa] Polimerase 1; PDE1: Phosphodiesterase 1; PHK: Phosphorylase Kinase; PKA: Protein Kinase A; PKC: Protein Kinase C; PLC: Phospholipase C; PLN: Phospholamban; PMCA: Plasma Membrane Calcium ATPase; PMCA: Plasma Membrane Calcium ATPase; PPARG: Peoxisome Proliferator Activation Receptor Gene; PPI: Protein-Protein Interaction; PRKCD: Protein Kinase C Type Delta; ROC: Regulator of Cullins; RTK: Receptor Tyrosine Kinase; RYR: Ryanodine Receptor 1; SERCA: Sarcoplasm Reticulum/Endoplasm Ca²⁺-ATPase; SERCA2a: Sarcoplasmic Reticulum Calcium Adenosine Triphosphatase; SIRT3: Sirtuin 3; SPP1: Secreted Phosphoprotein 1; STAT1: Signal Transducer And Activator of Transcription 1; STAT3: Signal Transducer and Activator of Transcription 3; STIM1: Stromal Interaction Molecule 1; TCR: T-Cell Receptor; TGF: Transforming Growth Factor; TGFB: Transforming Growth Factor-Beta; THBD: Thrombomodulin; TLR2: Toll Like Receptor 2; TNF: Tumor Necrosis Factor; TNNI3: Troponin I3; TPC: Tetrapac; TRDN: Triadin; VDAC1: Voltage-Dependent Anion-Selective Channel 1; VEGFA: Vascular Endothelial Growth Factor; XDH: Xanthine Dehydrogenase; VOCs: Voltage-Operated Channels; ROCs: Receptor-Operated Channels, NMDA: N-Methyl-D-Aspartate Receptors; SMOCs: Second-Messenger-Operated Channels; SOCs: Store-Operated Channels; ER/SR: Endoplasmic/Sarcoplasmic Reticulum; IP3Rs: Inositol-1,4,5-Trisphosphate Receptors; RYRs: Ryanodine Receptors; PLC beta, delta, epsilon, gamma and zeta: Phospholipase C; cADPR: Cyclic ADP-Ribose; NAADP: Nicotinic Acid Adenine Dinucleotide Phosphate; TnC: Troponin C.

Figure 5. Molecular docking and molecular dynamic interaction stability of EGCG, CGA, curcumin, and metformin upon binding with AGTR1.

(A) The 3D and 2D view of the binding interaction between EGCG, CGA, curcumin, and metformin with AGTR1. Blue ribbons represent the AGTR1, while green spheres represent the ligands. In the 2D view of interaction, amino acids are presented as circle plates with different colors representing the interaction chemistry. Complex stability is visualized in the RMSD of atom backbone **(B)**, while the RMSF determines the stability of the AGTR1 according to the fluctuation of its residues **(C)**. The stability of the compounds' structure was demonstrated as the RMSD of ligand conformation **(D)**, while the ligand movement describes the relative position of ligand movement during the simulation periods compared to the initial state **(E)**.

AGTR1: Angiotensin II Receptor Type 1; CGA: Chlorogenic Acid; EGCG: Epigallocatechin Gallate; RMSD: Root-Mean-Square Deviation; RMSF: Root-Mean-Square Fluctuation.

On the other hand, myocytes from MetS rats treated with the antioxidant N-acetylcysteine showed normal ROS levels and SERCA2a- mediated Ca^{2+} reuptake as well as accelerated cytosolic Ca^{2+} removal (Balderas-Villalobos et al., 2013). Previous work from Qin et al. (2012; 2014) provided data that the upregulation of NOX_2 and oxidation of SERCA2a found in C57BL/6 J mice, followed by the development of left ventricular hypertrophy and diastolic dysfunction (Calvert, 2014). Moreover, the critical role of NOX_2 in the modulation of SERCA2a expression could be explained by a study from Valdes et al. (2018), who demonstrated a NOX-dependent influence on Ca^{2+} handling proteins and myofibrils in rats aging myocytes.

Numerous studies have reported the beneficial effect of consuming natural products as a prevention or supportive treatment of metabolic syndrome (Firzan et al., 2023; Tabatabaei-Malazy et al., 2015; Villarroel-Vicente et al., 2021). There are several ways to process natural products to elicit health benefits, such as functional food or as a dietary supplement. The use of coffee and tea in cardiovascular effects has been revealed in many studies. Lukitasari et al. (2020) were the first to show a higher improvement of metabolic profile was seen in rats in the MetS model treated with a combination of coffee and tea than in single coffee or single green tea extract. The report showed that coffee and tea infusions could lower blood pressure, improve lipid profile, and increase the peroxisome proliferator-activated receptor gamma (PPARγ) and mitogen-activated protein kinase (MAPK) expression (Lukitasari et al., 2020). Moreover, the combination of coffee and green tea was shown to have a synergistic effect on the macrophage cell line and could inhibit the establishment of foam cells as an early marker of atherosclerosis (Rachmawati et al., 2021; 2022).

This present study was supported by previous reports demonstrating the anti-inflammatory and anti-oxidant properties of curcumin or EGCG to inhibit the progression of cardiac dysfunction due to MetS. Furthermore, the improvement of cardiomyocyte structure and cardiac interstitial fibrosis were also revealed with the administration of curcumin or EGCG. However, these reports did not mention the signaling pathway that is responsible for the cardioprotective effect in rats' MetS model. Our *in silico* analysis showed several receptors like RAGE and AGTR1 might be essential in Ca-handling abnormalities. The burst of inflammation and oxidative stress through metabolic dysfunction might be facilitated by AGTR1 (Akasaka et al., 2006; Fung et al., 2011). AGTR1 is a transmembrane receptor that regulates the pleiotropic process based on the KEGG database and several reports that involved NADPH oxidase, ROS, NF-κB, TNFα, IL-6, and SERCA2a. Interestingly, the binding affinities of EGCG, CGA, and curcumin were more negative than metformin from molecular docking analysis. Moreover, data from molecular dynamic studies showed that the binding was stable.

However, our work has several limitations. We only assessed markers of inflammation, NADPH oxidase, and SERCA2a at the transcriptional level. This study did not observe other vital proteins that play in the calcium handling mechanism, like RyR, **p**hospholamban, and NaCaATPase. Therefore, further research should measure the effect of coffee, green tea, and turmeric combinations on the calcium homeostasis marker at all levels, either transcriptionally or translationally. The cardiac structure abnormality should also be investigated for a better understanding of the cardioprotective effect of this combination. The LC-HRMS report should be validated using standard markers in future studies. A wet experimental study should accomplish molecular docking and molecular dynamic analysis.

CONCLUSION

The coffee, green tea, and turmeric might prevent heart dysfunction in MetS through modulation of oxidative stress and inflammation. The combination of coffee, green tea, and turmeric could be developed as a dietary product or supplement therapy for MetS disease to prevent cardiac complications.

CONFLICT OF INTEREST

The authors declare no conflicts of interest.

ACKNOWLEDGMENTS

REFERENCES

Akasaka H, Katsuya T, Saitoh S, Sugimoto K, Fu Y, Takagi S, Ohnishi H, Rakugi H, Ura N, Shimamoto K, Ogihara T (2006) Effects of angiotensin II type 1 receptor gene polymorphisms on insulin resistance in a Japanese general population: the Tanno-Sobetsu study. Hypertens Res 29(12): 961–967. https://doi.org/10.1291/hypres.29.961

Alshehri AM (2010) Metabolic syndrome and cardiovascular risk. J Community Med 17(2): 73–78. https://www.ncbi.nlm.nih.gov/pmc/articles/PMC3045098/

Balderas-Villalobos J, Molina-Muñoz T, Mailloux-Salinas P, Bravo G, Carvajal K, Gómez-Viquez NL (2013) Oxidative stress in cardiomyocytes contributes to decreased SERCA2a activity in rats with metabolic syndrome. Am J Physiol Heart Circ Physiol 305(9): H1344–H1353. https://doi.org/10.1152/ajpheart.00211.2013

Battault S, Renguet E, van Steenbergen A, Horman S, Beauloye C, Bertrand L (2020) Myocardial glucotoxicity: Mechanisms and potential therapeutic targets. Arch Cardiovasc Dis 113(11): 736–748. https://doi.org/10.1016/j.acvd.2020.06.006

Bhatti SN, Li JM (2020) Nox2 dependent redox-regulation of Akt and ERK1/2 to promote left ventricular hypertrophy in dietary obesity of mice. Biochem Biophys Res Comm 528(3): 506–513. https://doi.org/10.1016/j.bbrc.2020.05.162

Burnier M, Egan BM (2019) Adherence in hypertension: A review of prevalence, risk factors, impact, and management. Circ Res 124(7): 1124–1140. https://doi.org/10.1161/CIRCRESAHA.118.313220

Calvert JW (2014) Nox2 targets SERCA in response to a high fat high sugar diet. J Mol Cell Cardiol 72: 228–230. https://doi.org/10.1016/j.yjmcc.2014.03.018

de Geest B, Mishra M (2022) Role of oxidative stress in diabetic cardiomyopathy. Antioxidants (Basel) 11(4): 784. https://doi.org/10.3390/antiox11040784

D'Oria R, Schipani R, Leonardini A, Natalicchio A, Perrini S, Cignarelli A, Laviola L, Giorgino F (2020) The role of oxidative stress in cardiac disease: From physiological response to injury factor. Oxid Med Cell Longev 2020: 5732956. https://doi.org/10.1155/2020/5732956

Esmaeelpanah E, Razavi BM, Hosseinzadeh H (2021) Green tea and metabolic syndrome: A 10-year research update review. Iran J Basic Med Sci 24(9): 1159–1172. https://doi.org/10.22038/ijbms.2021.52980.11943

Ferreira LG, Dos Santos RN, Oliva G, Andricopulo AD (2015) Molecular docking and structure-based drug design strategies. Molecules 20(7): 13384–13421. https://doi.org/10.3390/molecules200713384

Firzan N, Andri F, Sukamto SM, Andi DP, Mirnawati S, Deepak C, Talha BE, Jesus S (2023) Natural products targeting inflammation-related metabolic disorders: A comprehensive review. Heliyon 9: 6. https://doi.org/10.1016/j.heliyon.2023.e16919

Fung MM, Rao F, Poddar S, Mahata M, Khandrika S, Mahata SK, O'Connor DT (2011) Early inflammatory and metabolic changes in association with AGTR1 polymorphisms in prehypertensive subjects. Am J Hypertens 24(2): 225–233, https://doi.org/10.1038/ajh.2010.210

Gogoi B, Chowdhury P, Goswami N, Gogoi N, Naiya T, Chetia P (2021) Identification of potential plant based inhibitor against viral proteases of SARS CoV 2 through molecular docking, MM PBSA binding energy calculations and molecular dynamics simulation. Mol Divers 25(3): 1963–1977. https://doi.org/10.1007/s11030-021-10211-9

Khan H, Ullah H, Nabavi SM (2019) Mechanistic insights of hepatoprotective effects of curcumin: Therapeutic updates and future prospects. Food Chem Toxicol 124: 182–191. https://doi.org/10.1016/j.fct.2018.12.002

Khan I, Rahman H, Abd El-Salam NM, Tawab A, Hussain A, Khan TA, Khan UA, Qasim M, Adnan M, Azizullah A, Murad W, Jalal A, Muhammad N, Ullah R (2017) Punica granatum peel extracts: HPLC fractionation and LC MS analysis to quest compounds having activity against multidrug resistant bacteria. BMC Complement Alternat Med 17(1): 247. https://doi.org/10.1186/s12906-017-1766-4

Kucera O, Mezera V, Moravcova A, Endlicher R, Lotkova H, Drahota Z, Cervinkova Z (2015) In vitro toxicity of epigallocatechin gallate in rat liver mitochondria and hepatocytes. Oxid Med Cell Longev 2015: 476180. https://doi.org/10.1155/2015/476180

Lau SO, Georgousopoulou EN, Kellett J, Thomas J, McKune A, Mellor D, Roach PD, Naumovski N (2016) The effect of dietary supplementation of green tea catechins on cardiovascular disease risk markers in humans: A systematic review of clinical trials. Beverages 2(2): 16. https://doi.org/10.3390/beverages2020016

Lukitasari M, Nugroho D, Rohman M, Widodo N, Farmawati A, Hastuti P (2020) Beneficial effects of green coffee and green tea extract combination on metabolic syndrome improvement by affecting AMPK and PPAR-α gene expression. J Adv Pharm Technol Res 11(2): 81–85. https://doi.org/10.4103/japtr.JAPTR_116_19

Ly LD, Xu S, Choi SK, Ha CM, Thoudam T, Cha SK, Wiederkehr A, Wollheim CB, Lee IK, Park KS (2017) Oxidative stress and calcium dysregulation by palmitate in type 2 diabetes. Exp Mol Med 49: e291. https://doi.org/10.1038/emm.2016.157

Pan Y, Wang Y, Zhao Y, Peng K., Li W, Wang Y, Zhang J, Zhou S, Liu Q, Li X, Cai L, Liang G (2014) Inhibition of JNK phosphorylation by a novel curcumin analog prevents high glucose-induced inflammation and apoptosis in cardiomyocytes and the development of diabetic cardiomyopathy. Diabetes 63(10): 3497–3511. https://doi.org/10.2337/db13-1577

Patti AM, Al-Rasadi K, Giglio RV, Nikolic D, Mannina C, Castellino G, Chianetta R, Banach M, Cicero AFG, Lippi G, Montalto G, Rizzo M, Toth PP (2018) Natural approaches in metabolic syndrome management. Arch Med Scie 14(2): 422–441. https://doi.org/10.5114/aoms.2017.68717

Qin F, Siwik DA, Luptak I, Hou X, Wang L, Higuchi A, Weisbrod RM, Ouchi N, Tu VH, Calamaras TD, Miller EJ, Verbeuren TJ, Walsh K, Cohen RA, Colucci WS (2012) The polyphenols resveratrol and S17834 prevent the structural and functional sequelae of diet-induced metabolic heart disease in mice. Circulation 125: 1757–1764. https://doi.org/10.1161/CIRCULATIONAHA.111.067801

Qin Z, Hou X, Weisbrod RM, Seta F, Cohen RA, Tong X (2014) Nox2 mediates high fat high sucrose diet-induced nitric oxide dysfunction and inflammation in aortic smooth muscle cells. J Mol Cell Cardiol 72: 56-63. http://doi.org/10.1016/j.yjmcc.2014.02.019

Rachmawati E, Rohman MS, Sargowo D, Kalsum U, Lyrawati D, Lukitasari M (2021) Decaffeinated coffee and green tea extract inhibit foam cell atherosclerosis by lowering inflammation and improving cholesterol influx/efflux balance through upregulation of PPARγ and miR-155. F1000Research 10: 1175. https://doi.org/10.12688/f1000research.74198.1

Rachmawati E, Rohman MS, Sishartami LW, Sargowo D, Kalsum U (2022) In silico modelling, regulation of cell viability and anti atherosclerotic effect in macrophage by decaffeinated coffee and green tea extract. Pharmacogn J 14(1): 46–55. https://doi.org/10.5530/pj.2022.14.7

Rohman MS, Lukitasari M, Nugroho AD, Nashi W, Nugraheini NIP, Sardjono WT (2017) Development of an experimental model of metabolic syndrome in Sprague Dawley rat. Res Jf Life Sci 4(1): 76–86. https://doi.org/10.21776/ub.rjls.2017.004.01.10

Saleh HA, Ramdan E, Elmazar MM, Azzazy HME, Abdelnaser A (2021) Comparing the protective effects of resveratrol, curcumin and sulforaphane against LPS/IFN-γ-mediated inflammation in doxorubicin-treated macrophages. Sci Rep 11(1): 545. https://doi.org/10.1038/S41598-020-80804-1

Shi Z, Zhu J X, Guo Y M, Niu M, Zhang L, Tu C, Huang Y, Li PY, Zhao X, Zhang ZT, Bai ZF, Zhang GQ, Lu Y, Xiao XH, Wang JB (2021) Epigallocatechin gallate during dietary restriction — potential mechanisms of enhanced liver injury. Front Pharmacol 11: 609378. https://doi.org/10.3389/fphar.2020.609378

Su G, Morris JH, Demchak B, Bader GD (2015) Biological network exploration with cytoscape 3. Curr Protoc Bioinformatics 47: 8.13.1-24. https://doi.org/10.1002/0471250953.bi0813s47

Szklarczyk D, Franceschini A, Wyder S, Forslund K, Heller D, Huerta-Cepas J, Simonovic M, Roth A, Santos A, Tsafou K P, Kuhn M, Bork P, Jensen LJ, von Mering C (2015) STRING v10: Protein-protein interaction networks, integrated over the tree of life. Nucleic Acids Res 43(D1): D447–D452. https://doi.org/10.1093/nar/gku1003

Tabatabaei-Malazy O, Larijani B, Abdollahi M (2015) Targeting metabolic disorders by natural products. J Diabetes Metab Disord 14: 57. https://doi.10.1186/s40200-015-0184-8

Tang WH, Cheng WT, Kravtsov GM, Tong XY, Hou XY, Chung SK, Sum S, Chung M, Chung SSM (2010) Cardiac contractile dysfunction during acute hyperglycemia due to impairment of SERCA by polyol pathway-mediated oxidative stress. Am J Physiol Cell Physiol 299: 643–653. https://doi.org/10.1152/ajpcell.00137.2010

Valdés Á, Treuer AV, Barrios G, Ponce N, Fuentealba R, Dulce RA, González DR (2018) NOX inhibition improves β-adrenergic stimulated contractility and intracellular calcium handling in the aged rat heart. Int J Mol Sci 19(8): 2404. https://doi.org/10.3390/ijms19082404

Villarroel-Vicente C, Gutiérrez-Palomo S, Ferri J, Cortes D, Cabedo N (2021) Natural products and analogs as preventive agents for metabolic syndrome via peroxisome proliferator-activated receptors: An overview. Eur J Med Chem 221: 113535. https://doi.org/10.1016/j.ejmech.2021.113535

Villegas S, Villarreal FJ, Dillmann WH (2000) Leukemia inhibitory factor and interleukin-6 downregulate sarcoplasmic reticulum Ca²⁺ ATPase (SERCA2) in cardiac myocytes. Basic Res Cardiol 95(1): 47–54. https://doi.org/10.1007/s003950050007

Wang M, Liu Y, Liang Y, Naruse K, Takahashi K (2021) Systematic understanding of pathophysiological mechanisms of oxidative stress-related conditions—diabetes mellitus, cardiovascular diseases, and ischemia– reperfusion injury. Front Cardiovasc Med 8: 649785. https://doi.org/10.3389/fcvm.2021.649785

Yu Z, Samavat H, Dostal AM, Wang R, Torkelson CJ, Yang CS, Butler LM, Kensler TW, Wu AH, Kurzer MS, Yuan JM (2017) Effect of green tea supplements on liver enzyme elevation: Results from a randomized intervention study in the United States. Cancer Prev Res (Phila) 10(10): 571–579. https://doi.org/10.1158/1940-6207.CAPR-17-0160

AUTHOR CONTRIBUTION:

Contribution	Rachmawati E	Rohman MS	Widodo N	Lukitasari M	Nugroho DA	Hermanto FE	Kholis MN
Concepts or ideas		x	x				
Design	x						
Definition of intellectual content	x	x	x				
Literature search	x						
Experimental studies	x			x	x		
Data acquisition	x			x	x		
Data analysis	x			x	x	x	
Statistical analysis	x						
Manuscript preparation	x	x	x	x	x	x	x
Manuscript editing		x	x			x	
Manuscript review	x	x	x	x	x	x	x